Application of FTIR Microspectroscopy to Monitor Biochemical Changes in Apoptotic Jurkat Cell Death Induced by Extract of *Pseuderanthemum palatiferum* Leaves

Benjawan Dunkhunthod[1], Benjamart Chitsomboon[2],
Suranaree University of Technology, Suranaree, Muang, Nakhon Ratchasima 30000
Kanjana Thummanu[3]
Synchrotron Light Research Institute (Public Organization), Suranaree, Muang, Nakhon Ratchasima 30000
and Patcharawan Sittisart[4*]
Sisaket Rajabhat University, Poe, Muang, Sisaket 33000

* *Corresponding Author: patcwan07@gmail.com*
[1] *Ph.D Student, School of Pre-clinic, Institute of Science.*
[2] *Assistant Professor, School of Biology, Institute of Science.*
[3] *Beamline Scientist, BL 4.1 IR Spectroscopy and Imaging.*
[4] *Assistant Professor, Division of Environmental Science, Faculty of Liberal Arts and Science.*

Article Info

Article History:
Received: January 20, 2020
Revised: July 29, 2020
Accepted: August 24, 2020

Keywords:
Pseuderanthemum palatiferum / Jurkat Cells / Normal Peripheral Blood Mononuclear Cells / Fourier-transform Infrared Spectroscopy / Apoptosis

Abstract

This study aimed to investigate cytotoxicity of *Pseuderanthemum palatiferum (P. palatiferum)* leave extract against Jurkat cells as compared to that against normal peripheral blood mononuclear cells (PBMCs). Fourier-transform infrared (FTIR) microspectroscopy was applied to evaluate biochemical changes in apoptotic Jurkat cell death. *P. palatiferum* leaves were extracted with 95% ethanol solution. Cytotoxicity of the extract on Jurkat cells and PBMCs were determined by 3-(4, 5-dimethylthiazol-2-yl)-2, 5-diphenyltetrazolium bromide (MTT) assay. The extract exhibited preferential cytotoxicity towards Jurkat cells but possessed lower toxicity against normal PBMCs when exposed to the same concentrations of the extract. Interestingly, the extract induced apoptotic cell death on Jurkat cells in both dose- and time-dependent manners as evidenced by the distribution of cytochrome C from mitochondria to cytosol. FTIR microspectroscopy confirmed the apoptosis-inducing activity of the extract towards Jurkat cells as indicated by the differences in the intensity of FTIR spectra bands in lipid and nucleic acid regions being responsible for discrimination of the mode of cell death. These findings may indicate that FTIR spectroscopy could be of potential use in identifying apoptotic cell death. Nevertheless, further biochemical assays should be performed to confirm the changes in FTIR spectra within lipid and nucleic acids regions.

การประยุกต์ใช้เทคนิค FTIR microspectroscopy ในการตรวจสอบการเปลี่ยนแปลงทางชีวเคมีของเซลล์มะเร็งเม็ดเลือดขาว (Jurkat) ที่ถูกเหนี่ยวนำการตายแบบอะพอพโตซิสด้วยสารสกัดใบฮว่านง็อก (*Pseuderanthemum palatiferum*)

เบญจวรรณ ดุนขุนทด[1] **เบ็ญจมาศ จิตรสมบูรณ์**[2]
มหาวิทยาลัยเทคโนโลยีสุรนารี ต.สุรนารี อ.เมือง จ.นครราชสีมา 30000
กาญจนา ธรรมนู[3]
สถาบันวิจัยแสงซินโครตรอน (องค์การมหาชน) ต.สุรนารี อ.เมือง จ.นครราชสีมา 30000
และ พัชรวรรณ สิทธิศาสตร์[4*]
มหาวิทยาลัยราชภัฏศรีสะเกษ ต.โพธิ์ อ.เมือง จ.ศรีสะเกษ 33000

** Corresponding Author: patcwan07@gmail.com*
[1] นักศึกษา สาขาวิชาปรีคลินิก สำนักวิชาวิทยาศาสตร์
[2] ผู้ช่วยศาสตราจารย์ สาขาวิชาชีววิทยา สำนักวิชาวิทยาศาสตร์
[3] นักวิทยาศาสตร์ประจำระบบลำเลียงแสงที่ 4.1: IR Spectroscopy and Imaging
[4] ผู้ช่วยศาสตราจารย์ สาขาวิชาวิทยาศาสตร์สิ่งแวดล้อม คณะศิลปศาสตร์และวิทยาศาสตร์

ข้อมูลบทความ **บทคัดย่อ**

ประวัติบทความ :
รับเพื่อพิจารณา : 20 มกราคม 2563
แก้ไข : 29 กรกฎาคม 2563
ตอบรับ : 24 สิงหาคม 2563

คำสำคัญ :
Pseuderanthemum palatiferum / เซลล์มะเร็งเม็ดเลือดขาวชนิด Jurkat / เซลล์เม็ดเลือดชนิดนิวเคลียสเดี่ยว / เทคนิค Fourier-transform infrared spectroscopy / การตายแบบอะพอพโตซิส

การศึกษาครั้งนี้มีวัตถุประสงค์เพื่อเปรียบเทียบความเป็นพิษของสารสกัดใบฮว่านง็อก (*Pseuderanthemum palatiferum*) ต่อเซลล์มะเร็งเม็ดเลือดขาวชนิด Jurkat และเซลล์เม็ดเลือดชนิดนิวเคลียสเดี่ยว (PBMCs) นอกจากนี้ยังใช้เทคนิค Fourier-transform infrared (FTIR) microspectroscopy เพื่อประเมินการเปลี่ยนแปลงทางชีวเคมีของเซลล์ที่ถูกเหนี่ยวนำการตายแบบอะพอพโตซิสอีกด้วย ทั้งนี้สกัดใบฮว่านง็อกด้วยสารละลาย 95% เอทานอล จากนั้นนำมาทดสอบความเป็นพิษต่อเซลล์มะเร็งเม็ดเลือดขาวชนิด Jurkat และเซลล์ PBMCs ด้วยเทคนิค 3-(4, 5-dimethylthiazol-2-yl)-2, 5-diphenyltetrazolium bromide (MTT) จากการทดสอบพบว่าสารสกัดแสดงความเป็นพิษเจาะจงต่อเซลล์มะเร็งเม็ดเลือดขาวชนิด Jurkat แต่แสดงความเป็นพิษน้อยกว่าในเซลล์ PBMCs เมื่อบ่มด้วยสารสกัดที่ความเข้มข้นเดียวกัน นอกจากนี้ยังพบว่าสารสกัดสามารถเหนี่ยวนำการตายแบบอะพอพโตซิสต่อเซลล์มะเร็งเม็ดเลือดขาวชนิด Jurkat ซึ่งพิจารณาได้จากการกระจายตัวของไซโตโครมซีจากไมโทคอนเดรียไปยังไซโทซอล ผลการวิเคราะห์ด้วยเทคนิค FTIR microspectroscopy ยืนยันฤทธิ์ของสารสกัดในการเหนี่ยวนำการตายแบบอะพอพโตซิสของเซลล์เม็ดเลือดขาวชนิด Jurkat โดยพิจารณาจากค่าความแตกต่างของสเปกตรัมของ FTIR ที่มีความสัมพันธ์กับปริมาณของไขมันและกรดนิวคลีอิกภายในเซลล์ จากการค้นพบนี้อาจบ่งชี้ได้ว่าเทคนิค FTIR microspectroscopy อาจเป็นประโยชน์ในการระบุการตายแบบอะพอพโตซิสของเซลล์ อย่างไรก็ตามในอนาคตควรตรวจวิเคราะห์ทางชีวเคมีเพิ่มเติมเพื่อยืนยันการเปลี่ยนแปลงของสเปกตรัม FTIR ในช่วงของไขมันและกรดนิวคลีอิก

1. Introduction

The global burden of cancer continues to increase largely because of the aging people and growth of the world population along with an increasing adoption of cancer causing behaviors, particularly smoking. In Thailand, there were about 170,495 new diagnosed cancer cases and about 114,199 cancer deaths in 2018 as reported by GLOBOCAN [1]. Several chemotherapeutic agents are used for cancer treatment but there is still the problem of selective toxicity and severe side effects. Therefore, there is an immediate need to discover alternative anticancer agents. Many researchers have focused on identifying therapeutic effects of natural products that selectively induce apoptosis and growth arrest in cancer cells without cytotoxic effects on normal cells [2].

Pseuderanthemum palatiferum (Nees) Radlk. (*P. palatiferum*) or Hoan-Ngoc is considered as a new medicinal plant in folk medicine for both treatment and prevention of many diseases including cancer. Several studies have described the beneficial effects of *P. palatiferum* such as antioxidants, antidiabetic, anti-inflammatory, hypotensive, anti-angiogenesis, and anti-proliferative activities [2-7]. *P. palatiferum* leaves have been reported to contain many important compounds such as flavanoids, apigenin, stigmasterol, *β*-sitosterol, *β*-sitosterol-3-0-*β*-glucoside, and apigenin-7-0-*β*-glucoside [8-9]. These compounds have been reported to have anticancer properties by inhibiting *in vitro* proliferation of human breast MCF-7 and MDA-MB-231 adenocarcinoma cells [10-11] and induce apoptosis in murine fibrosarcoma MCA-102 cells [12]. Our previous study reported that cytotoxicity of 95% ethanolic extracts of *P. palatiferum* (EEP) was mediated through apoptotic mechanism as evidenced by the nuclear condensation and DNA laddering fragmentation [13]. Nonetheless, the differential susceptibility of Jurkat cells to EEP-induced cytotoxicity compared to normal cells has never been investigated. Therefore, it is necessary to assess the selective cytotoxic effects of EEP against Jurkat cells compared with normal cells.

Detection of apoptotic cell death can be performed by several assays that analyze either morphological changes or distinct biochemical events occurring during programmed cell death by observing nuclear morphology changes by Hoechst staining, analyzing DNA fragmentation by gel electrophoresis, detecting cytochrome C release by flow cytometry, and detecting phosphatidylserine externalization by annexinV-PI staining [14-17]. Nonetheless, the aforementioned methods are used to monitor for alterations in apoptotic cells which each requires specific reagents, complicated handling of samples and/or highly skilled personnel.

Currently, Fourier-transform infrared (FTIR) microspectroscopy has been applied to study the biochemical alteration in various biological samples [18, 19]. This technique presents several advantages, such as sensitivity, rapidity, and no requirement for staining or reagents [20]. FTIR microspectroscopy might therefore be adapted as an alternative method for assessing the biochemical alteration in apoptotic and necrotic cell death of cancer cells.

Our study aimed to investigate the differential sensitivity of Jurkat cells to EEP-induced cytotoxicity compared to normal peripheral blood mononuclear cells (PBMCs). In order to confirm the apoptosis-inducing activities of EEP, FTIR microspectroscopy was applied to evaluate the biochemical changes observed in Jurkat cells.

2. Materials and Methods

2.1 Plant material

P. palatiferum was purchased from Yasothon

province, Thailand. The specimen was identified by Dr.Kongkanda Chayamarit of forest Herbarium, Royal Forest Department, Bangkok, Thailand. A voucher specimen (BKF 174009) was deposited at the Forest Herbarium, Royal Forest Department, Bangkok, Thailand.

2.2 Preparation of 95% ethanol extract of *P. palatiferum* leaves

The preparation of 95% ethanol extract of *P. palatiferum* leaves (EEP) was described by Sittisart and Chitsomboon [6]. Briefly, fresh leaves (4 kg) were blended in 16 L of 95% ethanol and filtered through gauze. The extract was centrifuged at 3,500×*g* for 10 min, and then the supernatant was filtered through a Whatman No.1 filter paper. After that, the ethanolic filtrate was concentrated using a vacuum rotary evaporator (Buchi Labortechnik AG, Flawil, Switzerland) and dried by lyophilization (Freeze-Zone 12 plus, Labconco Corporation, Missouri, USA) into powder of 95% ethanol crude extract (87.63 g). The extract was stored at -20°C and dissolved in DMSO for use in the experiments.

2.3 Cell culture

Jurkat leukemic cell line was purchased from Cell Line Services (CLS), Germany. Human normal peripheral blood mononuclear cells (PBMCs) were obtained from buffy coat, which were kindly provided by Blood Bank of Maharat Nakhon Ratchasima Hospital Nakhon Ratchasima province, Thailand.

Jurkat cells and PBMCs were cultured in RPMI-1640 supplemented with 10% FBS, 100 U/mL penicillin and 100 µg/mL streptomycin. All cell lines were maintained at 37°C in 5% CO_2 and 95% humidity.

2.4 Isolation of normal peripheral blood mononuclear cells (PBMCs)

Buffy coat was isolated by Biocoll separating solution, density 1.077 g/mL. Briefly, 7 mL of buffy coat was added to a 15 mL conical tube. The buffy coat was diluted with an equal volume of PBS and then carefully laid onto the Biocoll separating solution. The tube was centrifuged without a brake at 400×*g* for exactly 30 min at 25°C. The layer of PBMCs between the plasma and Biocoll separating solution was collected and washed twice with PBS (centrifuged at 400×*g* for 5 mins). This study was approved by ethics committee for researchers involving human subjects (In case of minimal risk review) of Suranaree University of Technology (Project code: EC-57-04).

2.5 *In vitro* cytotoxic test (MTT assay)

The cytotoxic effect of EEP on cell proliferation was determined by 3-(4, 5-dimethylthiazol-2-yl)-2,5-diphenyltetrazolium bromide (MTT) assay [6]. Jurkat cells and PBMCs were seeded in a 96-well plate at a density of 2.5×10^4 and 2×10^6 cells/well, respectively. The cells were allowed to adhere overnight, and then treated with various concentrations of EEP for 24 hrs. After incubation, the cell viability was evaluated by MTT assay.

$$\text{Percent of cell viability} = \frac{\text{Average OD for test group}}{\text{Average OD for control group}} \times 100$$

2.6 Cytochrome C release

The release of cytochrome C, a key mitochondrial protein, is an important hallmark in apoptotic pathway and is considered as a point of no return in the apoptosis process. The levels of cytochrome C in mitochondria can be detected by directly probing with anti-cytochrome C-FITC and analyzed by a flow

cytometer. After treatment, Jurkat cells were collected and washed twice with PBS. Then, the cell pellets were prepared at a density of 1×10^6 cells in 200 µL of PBS and then stained by using Millipore's FlowCellectTM Cytochrome C kit (Millipore, USA). The stained cells were analyzed by flow cytometry (BD FACS Calibur with Cell Quest Pro software).

2.7 FTIR microspectroscopy

After treatment, Jurkat cells were collected and washed twice with 0.85% NaCl. Cell pellets were dropped onto low-e microscope slides (MirrIR, Kevley Technologies) and vacuum dried for 30 min in a desiccator to eliminate the excess water. The dried cells were kept in a desiccator until FTIR analysis.

FTIR spectra were recorded using a FTIR microspectroscopy equipment, at the Synchrotron Light Research Institute (Public Organization), Thailand. FTIR spectra were acquired with a Bruker Vertex 70 spectrometer coupled with a Bruker Hyperion 2000 microscope (Bruker Optics Inc., Ettlin-gen, Germany) - equipped with a nitrogen cooled MCT (HgCdTe) detector with a 36 × IR. The spectra were obtained in the reflection mode covered spectral range of 4000-600 cm^{-1}, using an aperture size of 50 µm × 50 µm, with a resolution of 6 cm^{-1}. Each spectrum was collected at 64 scans. OPUS 7.2 software (Bruker Optics Ltd, Ettlingen, Germany) was used to acquire FTIR spectral data and control instrument system.

The spectra of non-treated cells, etoposide- and EEP-treated cells were identified by Principal Component Analysis (PCA) using variability of the Unscrambler 9.7 software (CAMO Software AS, Oslo, Norway). Absorbance spectra were acquired in the spectral range of 3000-2800 cm^{-1} (Lipid regions) and 1300-850 cm^{-1} (Nucleic acid regions). The preprocessing of the spectra was performed by second derivative transformations using Savitzky-Golay algorithm (nine smoothing points) and normalized with extended multiplicative signal correction (EMSC). Second derivative and vector normalization were applied to compensate for differences in sample thickness, minimize baseline variation and provide better visual identification of the band in the raw spectra that overlapped each other. Score plots (2D) and loading plots were used to represent the different classes of data and relations among variables of data set, respectively. The integrated peak areas of second derivative spectra were analyzed using OPUS 7.2 software (Bruker) with a spectral range of 3000-2800 cm^{-1} and 1300-850 cm^{-1}.

2.8 Statistical analysis

All statistical significances (Statistics Package for the Social Sciences, version 11) were determined by performing a One Way Analysis of Variance (ANOVA) with a *post-hoc* Tukey's analysis to determine differences between the mean values of multiple groups. Values were considered statistically significant when $p<0.05$ and data were representative of at least three independent experiments.

3. Results and Discussion

3.1 Extraction yield

P. palatiferum or Hoan-Ngoc fresh leaves were extracted by 95% ethanol to obtain a final yield of 2.91% (w/w) EEP.

3.2 Cytotoxic effect of EEP against normal peripheral blood mononuclear cells (PBMCs) compared Jurkat cells

The *in vitro* cytotoxic effect of EEP against Jurkat cell lines compared to peripheral blood mononuclear cells, PBMCs (normal cells) after 24 hrs of exposure are shown in Figure 1. The results showed

that Jurkat cell lines exhibited different susceptibilities to EEP in a dose-dependent manner. These results are consistent with our previous study, we reported that Jurkat cells exhibited the most sensitive in terms of cytotoxicity to EEP [13]. The results in this study agreed with several previous reports which showed the cytotoxic effects of *P. palatiferum* crude extracts against different cancer cell lines such as colon cancer cell lines; HCT15, SW48, SW480 [21], colon cancer cells (Caco2) and breast cancer cell lines (MCF-7) [5]. Interestingly, EEP inhibited cell growth on Jurkat cells with an IC_{50} of 476.35±31.51 µg/mL, 3 fold greater than that of PBMCs (IC_{50}=1431.03±78.25 µg/mL). These results indicated that EEP showed higher anti-proliferative activity towards Jurkat cell lines than PBMCs. Importantly, a great desired property of chemotherapeutic compounds is the selective cytotoxicity against cancer cells with less cytotoxic effect to normal cells for avoiding side effects to healthy tissues. However, cell death largely occurs through either of two distinct processes: necrosis or apoptosis [22]. Consequently, it is necessary to distinguish apoptotic from necrotic cell death whether the cytotoxic effect of EEP was mediated through the apoptotic mechanism.

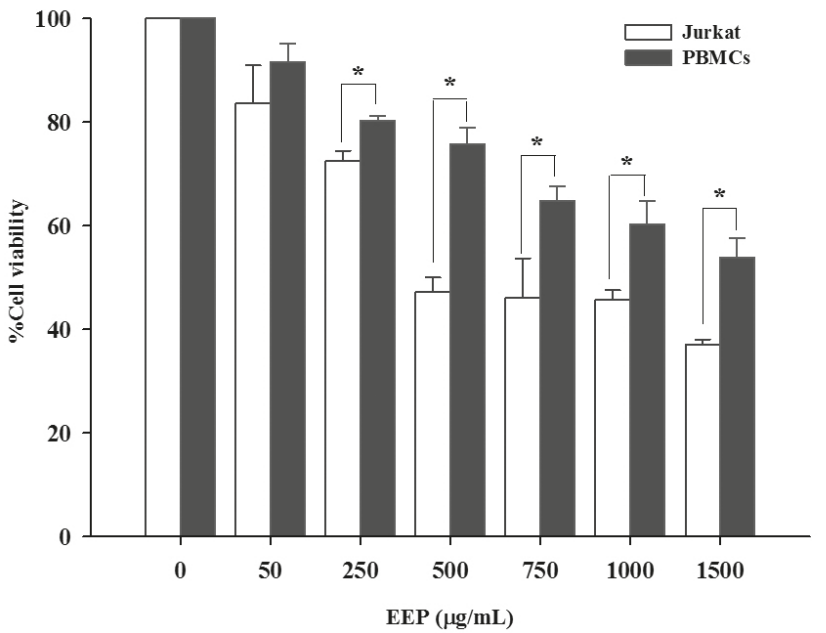

Figure 1 Cytotoxic effects of EEP against Jurkat cell lines compared to normal human peripheral blood mononuclear cells (PBMCs). Cells were exposed to various concentrations of EEP for 24 hrs prior to assessment of cell viability by MTT assay. Values are expressed as mean± SD (n = 4) of a representative of three independent experiments with similar result. Statistical analysis was performed by Student's t-test. * indicates significant differences between two groups (p<0.05).

3.3 Cytochrome C release

Cytochrome C is a protein that located in the space between the inner and outer mitochondrial membranes. During apoptotic process, the mitochondrial membrane, which is disrupted, caused the translocation of cytochrome C from mitochondria into cytosol. The levels of cytochrome C in mitochondria can be detected directly by probing with anti-cytochrome C-FITC and subsequently analyzed by flow cytometer. Therefore, the cells undergoing apoptosis demonstrated the reduction of FITC intensity in mitochondria, implicating the cytochrome C release. As shown in Figure. 2A-2D, EEP induced the release of cytochrome c from mitochondria into cytosol in both dose- and time-dependent manners. As suggested in Figure 2A and 2B, when compared to un-treated control cells, the mitochondrial cytochrome C release was significantly increased (p<0.05) by 10- and 11-fold after exposed to EEP at 300 and 600 µg/mL, respectively. Likewise, the time course study illustrated that the releasing of cytochrome C were significantly increased (p<0.05) about 7- and 10-fold after exposed to 300 µg/mL of EEP for 12 and 24 hrs, respectively Figure 2C and 2D. Interestingly, EEP at concentration of 300 and 600 µg/mL significantly induced the cytochrome C release higher (p<0.05) than etoposide-treated group. Findings obtained in this study showed that treatment of Jurkat cells with EEP increased cytochrome C release from mitochondria into cytosol. In the cytosol, cytochrome C interacts with adaptor protein apoptotic peptidase activating factor 1 (Apaf-1), and activates the downstream effector caspase-3 culminating in apoptotic cell death [23]. The findings of this study are consistent with earlier studies reporting the effect of EEP to trigger apoptotic cell death as evidenced by nuclear condensation and DNA fragmentation [13]. Kongprasom et al. [24] revealed that the aqueous extracts of *P. palatiferum* leaf exerted anti-cancer activity by suppression of cell viability and induction of ROS mediated mitochondrial dependent apoptosis in A549 cells. Therefore, the release of cytochrome C from the mitochondria into cytosol suggested that the extracts could induced apoptosis through a mitochondria-dependent pathway.

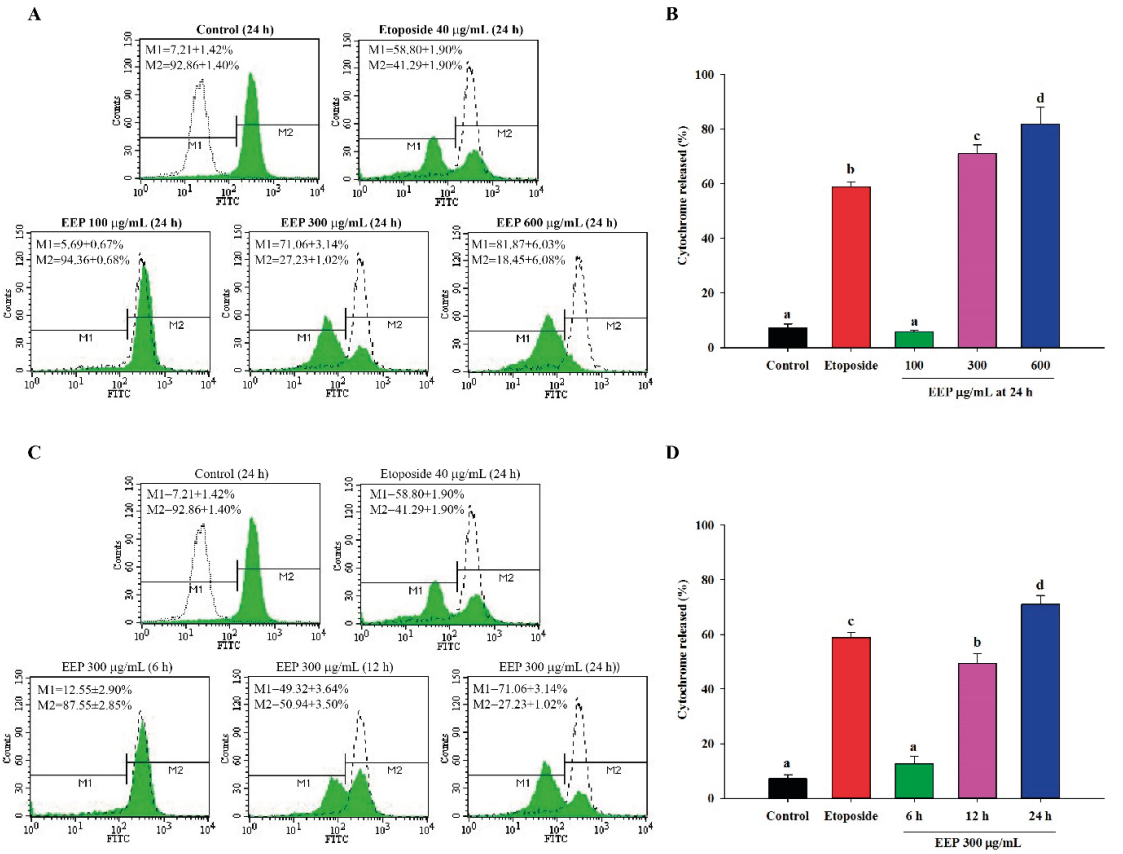

Figure 2 Flow cytometry analysis of cytochrome C release of Jurkat cells exposed to various concentrations of EEP for 24 h (A and B) and kinetics of apoptosis induction in Jurkat cells exposed to 300 μg/mL of EEP (C and D). Left panel shows the representative of flow cytometry analysis of three independent experiments. M1 region shows the progressive increase of non-fluorescent cell population and M2 region shows the decrease of highly fluorescent cell population. The reduction of fluorescent intensity in cell population implicates the release of cytochrome C from mitochondria into cytosol. Right panel represents the mean of percentages of cytochrome C release. Values are expressed as mean ± SD from three independent experiments. Bars marked with different letters (a, b, c, and d) are significantly different between groups at $p<0.05$ as determined by one-way ANOVA with Tukey's *post hoc* test.

3.4 Biochemical changing detected by FTIR microspectroscopy

FTIR microspectroscopy has been used as a powerful technique for studying apoptotic cell death. [3, 4]. This is the first report of an application of FTIR technique to evaluate biomolecule changes of Jurkat cell death induced by EEP.

Average of FTIR original spectra (3000-2800 cm^{-1} and 1800-800 cm^{-1}) of untreated control, etoposide- and EEP-treated cells are shown in Figure 3. The second derivative was accomplished for spectral analysis and a sharp absorption of individual peak of control and treated-cells was clearly identified. The second derivative spectra of the respective lipid region

(3000-2800 cm^{-1}) and nucleic acids region (1300-800 cm^{-1}) are presented in Figure 4A and 4B, respectively. The peak at 2922 cm^{-1} and 2852 cm^{-1}, corresponding mainly to CH_2 stretching modes of methylene chains in membrane lipids, exhibited a higher intensity in etoposide- and 600 µg/mL of EEP-treated cells when compared to untreated control cells. Moreover, four important IR bands (at 1240 cm^{-1}, 1084 cm^{-1}, 993 cm^{-1} and 966 cm^{-1}) due to various structure groups in DNA and RNA illustrated a decrease of nucleic absorbance in etoposide- and EEP-treated cells compared to untreated control cells. FTIR spectral changes that were detected due to EEP-induced apoptosis in Jurkat cells. The findings of this study are consistent with other reports where apoptosis is triggered by other compounds [18-20, 25]. To evaluate the change in lipid and nucleic acid content between five sample groups, the integrated area of the lipid and nucleic acid regions was calculated. Figure 5 illustrates the average of integrated areas of second derivative spectra in lipid regions (2971-2950 cm^{-1}, 2936-2913 cm^{-1}, 2878-2867 cm^{-1}, 2860-2845 cm^{-1} and 1748-1733 cm^{-1}) and nucleic acid regions (1060-1033 cm^{-1}, 996-988 cm^{-1}, 973-955 cm^{-1}, 919-950 cm^{-1} and 1864-847 cm^{-1}) of untreated, etoposide- and EEP-treated cells. The results showed that the percentages of integrated area of the lipids region in the etoposide- and EEP-treated cells displayed significantly less than the untreated control cells group ($p<0.05$). In contrast, the etoposide- and EEP-treated cells demonstrated a significant decrease in the percentages of nucleic acid areas compared to untreated control cells ($p<0.05$). Our findings are in agreement with a previous report on the actinomycin D which induced apoptosis in the lymphocyte Jurkat cell line, the lipid integral area (2800-3000 cm^{-1}) in apoptotic cells were greater than that of viable cells, whereas the decrease of lipid the integral area was observed in necrotic cells induced by lowering the pH value to 4.2 [26]. Machana et al. [19] reported an increase of the lipid regions (3000-2800 cm^{-1}, 1755-1710 cm^{-1}, and 1478-1350 cm^{-1}) in the melphalan-treated human leukemic U937 cells compared to the untreated U937 cells. An increase in lipid absorbance of apoptotic cells was related to membrane changes during apoptosis process such as the collapse of lipid membrane asymmetry causing the inside out exposure of phosphatidylserine to the outer leaflet of membrane, cell shrinkage, membrane blebbing and apoptotic body formation [26-27]. Consistent with our previous finding, the exposure of Jurkat cells to EEP induced morphological alterations whose common features include nuclear condensation, cell shrinkage and membrane blebbing implicated in apoptosis cell death [13]. By comparison, the decrease of lipid content in necrotic cells may be due to swelling of organelles and loss of plasma membrane integrity [18, 20]. Moreover, it could also be associated with permeabilization of mitochondrial outer membrane, resulting in cytochrome C and pro-apoptotic molecules release into cytosol [28]. Our results indicate that the nucleic acid content of EEP-treated cells showed a dramatic decrease in a dose-dependent manner. These findings support previous reports stating that the absorbance of nucleic acid region was reported to decrease in apoptotic cell death and by contrast, to increase in necrotic cell death [18-19, 27]. The apoptotic DNA absorbed less IR due to the opaqueness of DNA (non-Beer-Lambert absorption) caused by its condensation of DNA during apoptosis [29]. In addition, the decrease in DNA content may be related to the progress of internucleosomal DNA cleavage during apoptosis process [30].

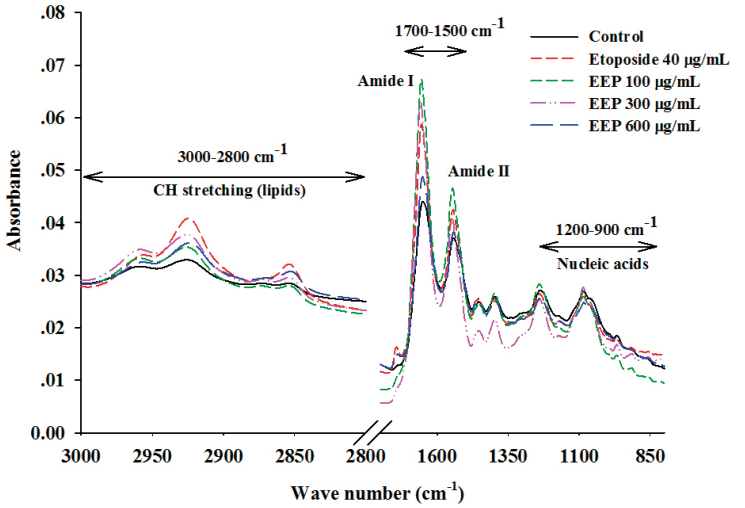

Figure 3 Average original FTIR spectra (*n*=426) obtained from control cells (*n*=50) and Jurkat cells exposed to EEP at 100 µg/mL (*n*=86), 300 µg/mL (*n*=45), 600 µg/mL (*n*=161), or 40 µg/mL of etoposide positive control (*n*=84) for 24 hrs.

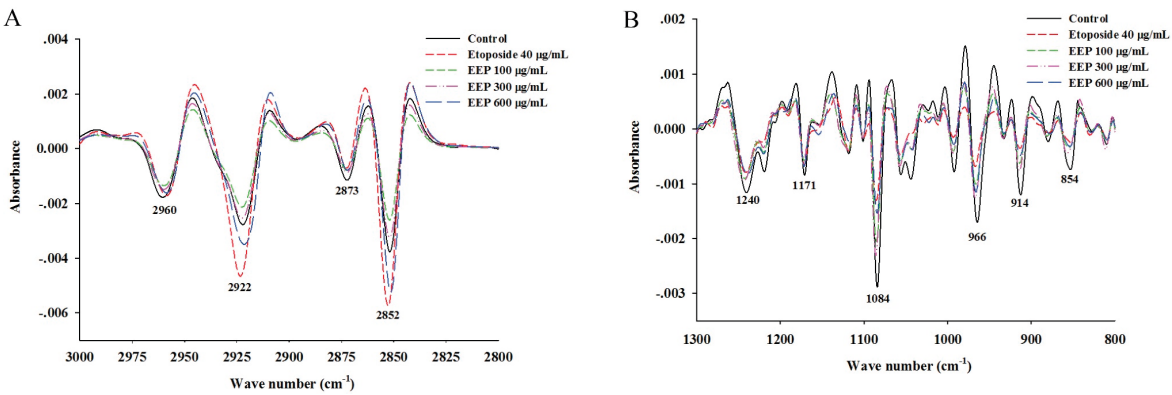

Figure 4 Average second derivative spectra of Jurkat control cells and Jurkat exposed to EEP at 100, 300, 600 µg/mL, and 40 µg/mL of etoposide positive control at 24 hrs after baseline and normalization with extended multiplicative signal correction (EMSC). The data were represented in two regions: (A) lipid regions (3000-2800 cm^{-1}) and (B) nucleic acid regions (1300-800 cm^{-1}).

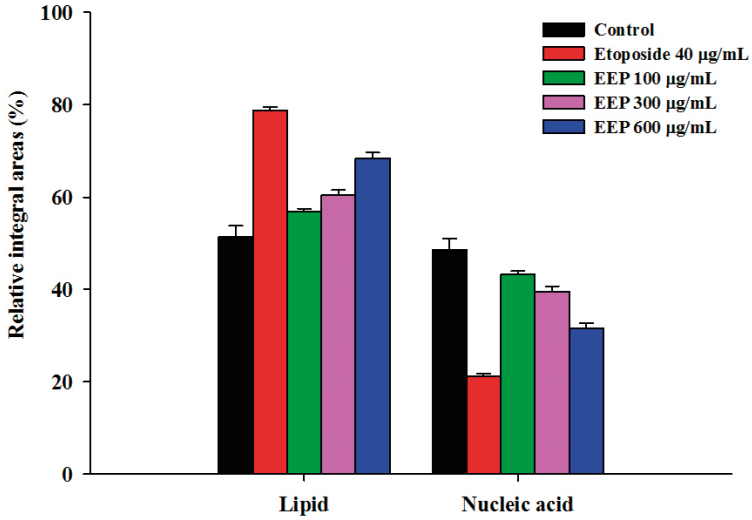

Figure 5 The percentages of integrated areas of second derivative spectra for remarkable lipid and nucleic acid regions of Jurkat control cells and Jurkat exposed to EEP at 100, 300, 600 µg/mL, and 40 µg/mL of etoposide positive control at 24 hrs. Data were calculated from normalized second derivative spectra. The differences between mean of the percentages of integrated areas were significantly difference among five groups by one-way ANOVA ($p< 0.05$). Data are represented as means ± SD. Bars marked with different letters (a, b, c, and d) are significantly different between groups at $p<0.05$ as determined by one-way ANOVA with Tukey's *post hoc* test.

The second derivative spectra of untreated cells, etoposide- and EEP-treated cells were further analyzed by principle component analysis (PCA). Two-dimensional PCA score plot was used to analyze major spectral variations between five sample groups (Figure 6A). PCA score plots demonstrated that the clusters of the highest concentration of EEP-treated cells (600 µg/mL) and etoposide-treated cells were separated from other groups along PC1 (55%). The cluster of etoposide- and EEP-treated (100 and 300 µg/mL) groups were distinguished from untreated control cells along PC2 by 16%. PCA loading plots were used to distinguish the variables of the spectrum, which most contributed to the clustering (Figure 6B). PC1 loading plot was discriminated by the positive loading spectra at 2923 cm^{-1} and 2852 cm^{-1} caused by C-H stretching, and the negative loading spectra at 1086 cm^{-1} resulting from PO_2-symmetric stretching vibrations of nucleic acid (RNA and DNA), which separated the negative score plot of EEP-treated cells (600 µg/mL) and etoposide-treated cells from the positive score plot of other cluster groups. Likewise, the discrimination along PC2 could be explained by the positive loading of PC2 in C-H stretching region (centered at 2916 cm^{-1} and 2850 cm^{-1}) and nucleic acid region (centered at 1082 cm^{-1}, 991 cm^{-1} 964 cm^{-1}, and 912 cm^{-1}), which separated the negative score plot of untreated control cells from the positive score plot of etoposide- and EEP-treated (100 and 300 µg/mL) groups. Based on the PCA analysis, the biochemical changes of EEP-induced apoptotic cell death in Jurkat cells associated with an increase of

lipids and a decrease of nucleic acids are responsible for discrimination of the mode of cell death. PCA analysis showed good results for classifying FTIR spectra of apoptotic cells versus viable cells [19, 25]. Pocasap et al. [31] investigated the chemopreventive potential of different compounds (sulforaphane, alyssin and iberin) in hepatocellular carcinoma cell HepG2 using SR-FTIR spectroscopy and PCA classification. Based on our finding, FTIR microspectroscopy can be used as an alternative method to identify biochemical profiles of apoptosis induction of the test compounds on cancer cells, which is of particular interest for the field of drug development to target many disease scenarios such as monitoring cancer cell alterations in the clinic. The advantages of this technique are a label-free, non-contact, and non-invasive technique for analysis of biochemical profiles in biological samples [32]. Since this method provides distinctive biochemical profiles and minimum handling of samples and limited reagents. However, in future studies, the combination of FTIR microspectroscopy and more biochemical assays are necessarily performed to confirm the changes in the FTIR spectra of lipid and nucleic acids regions.

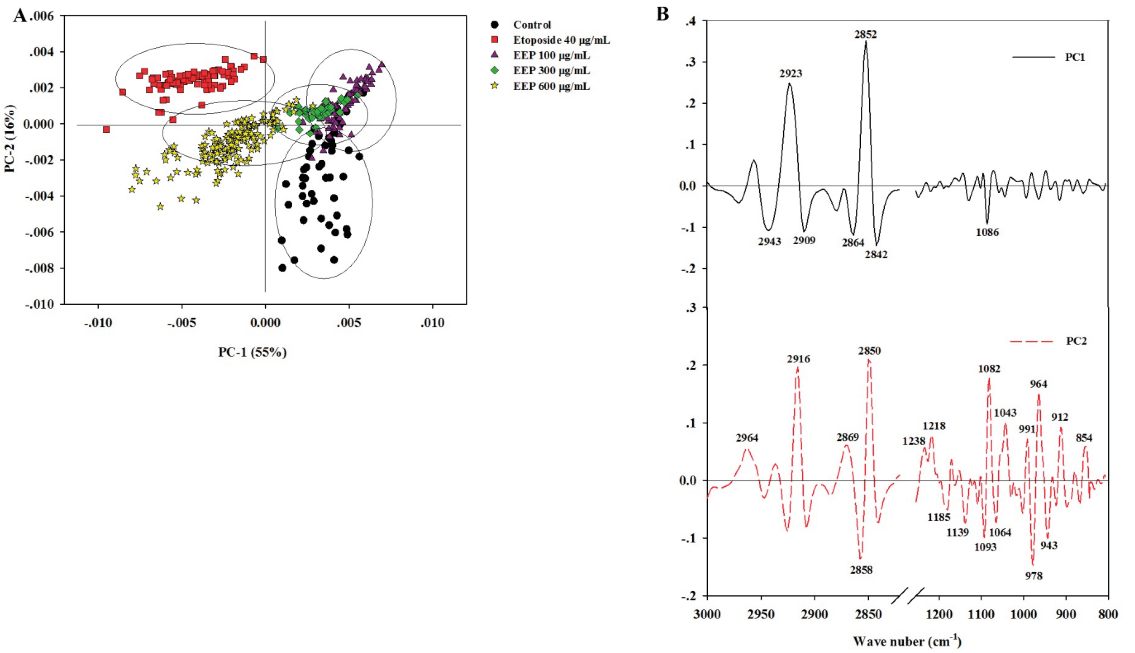

Figure 6 PCA analysis of FTIR spectral range 3000-800 cm^{-1} giving PCA score plot (A) and PCA loading plot (B). PCA score plots showed distinct clustering between Jurkat control cells and Jurkat exposed to EEP at 100, 300, 600 µg/mL, and 40 µg/mL of etoposide positive control at 24 hrs. PCA loading plots identify biomarker difference over spectral range of samples.

4. Conclusion

In conclusion, our findings suggest that EEP exhibited the preferential cytotoxicity towards Jurkat cells as less toxicity was obtained in normal PBMCs. EEP induced Jurkat cell death mediated through apoptosis as evidenced by the release of cytochrome C. FTIR spectra showed increased lipid content and decreased nucleic acid content which appeared to be attributable

to apoptotic process. This study reveals that FTIR spectroscopy allowed us to distinguish the mode of cell death. In addition, it can be helpful for evaluating biochemical profile of apoptotic cells. Further detailed study should be done for clarifying apoptosis induction mechanisms of the EEP against Jurkat cells.

5. References

1. Bray, F., Ferlay, J., Soerjomataram, I., Siegel, R.L., Torre, L.A. and Jemal, A., 2018, "Global Cancer Statistics 2018: GLOBOCAN Estimates of Incidence and Mortality Worldwide for 36 Cancers in 185 Countries," *CA: A Cancer Journal for Clinicians*, 68 (6), pp. 394-424.

2. Tsao, A.S., Kim, E.S. and Hong, W.K., 2004. "Chemoprevention of Cancer," *A Cancer Journal for Clinicians*, 54 (3), pp. 150-180.

3. Chayarop, K., Peungvicha, P., Wongkrajang, Y., Chuakul, W., Amnuoypol, S. and Temsiririrkkul, R., 2011, "Pharmacognostic and Phytochemical Investigations of *Pseuderanthemum palatiferum* (Nees) Radlk. ex Lindau Leaves," *Pharmacognosy Journal*, 3 (23), pp. 18-23.

4. Khonsung, P., Panthong, A., Chiranthanut, N. and Intahphuak, S., 2011, "Hypotensive Effect of the Water Extract of the Leaves of *Pseuderanthemum palatiferum*," *Journal of Natural Medicines*, 65 (3-4), pp. 551-558.

5. Phasuk, S. and Meeratana, P., 2014, "Cytotoxicity Activity of *Pseuderanthemum palatiferum* Crude Extracts against Breast and Colon Cancer Cells," *Thai Journal of Science and Technology*, 22 (6), pp. 848-860.

6. Sittisart, P. and Chitsomboon, B., 2014, "Intracellular ROS Scavenging Activity and Downregulation of Inflammatory Mediators in RAW264.7 Macrophage by Fresh Leaf Extracts of *Pseuderanthemum palatiferum*," *Evidence-Based Complementary and Alternative Medicine*, pp. 1-11.

7. Sala-ngam, B., Suksawaeng, S., Dunkhunthod, B. and Chitsomboon, B., 2014, "Anti-Angiogenesis of Hoan-Ngoc (*Pseuderanthemum palatiferum* (Nees) Radlk) Extract on B16F10-Inoculated CAM," *Proceedings of the 6th International Conference on Natural Products for Health and Beauty*, Khon Kaen, Thailand, pp. 110-114.

8. Diệu, H.K., 2008, "KHẢO SÁT THÀNH PHẦN HÓA HỌC CỦA LÁ XUÂN HOA (*Pseuderanthemum palatiferum*)," *Tạp chí Khoa học Trường Đại học Cần Thơ*, pp. 232-240.

9. Sittisart, P., Chitsomboon, B. and Kaminski, N.E., 2016, "*Pseuderanthemum palatiferum* Leaf Extract Inhibits the Proinflammatory Cytokines, TNF-α and IL-6 Expression in LPS-activated Macrophages," *Food and Chemical Toxicology*, 97, pp. 11-22.

10. Chai, J., Kuppusamy, U. and Kanthimathi, M., 2008, "Beta-sitosterol Induces Apoptosis in MCF-7 cells," *Malaysian Journal of Biochemistry and Molecular Biology*, 16 (2), pp. 28-30.

11. Awad, A., Chinnam, M., Fink, C. and Bradford, P., 2007, "*β*-Sitosterol Activates Fas Signaling in Human Breast Cancer Cells," *Phytomedicine*, 14 (11), pp. 747-754.

12. Moon, D.O., Lee, K.J., Choi, Y.H. and Kim, G.Y., 2007, "*β*-Sitosterol-induced-apoptosis is Mediated by the Activation of ERK and the Downregulation of Akt in MCA-102 Murine Fibrosarcoma Cells," *International immunopharmacology*, 7 (8), pp. 1044-1053.

13. Dunkhunthod, B. and Chitsomboon, B., 2014, "Antiproliferative Effect on Cancer Cells and Mutagenic Activity of *Pseuderanthemum palatiferum* (Nees) Radlk," *Proceedings of the 5th International Conference on Natural Products for Health and Beauty*, Phuket, Thailand, pp. 128-132.

14. Cohausz, O., Blenn, C., Malanga, M. and Althaus, F.R., 2008, "The Roles of Poly (ADP-Ribose)-Metabolizing Enzymes in Alkylation-Induced *Cell Death," Cellular and Molecular Life Sciences*, 65 (4), pp. 644-655.

15. Choi, E.J. and Kim, G.H., 2009, "Apigenin Induces Apoptosis through a Mitochondria/Caspase-Pathway in Human Breast Cancer MDA-MB-453 Cells," *Journal of Clinical Biochemistry and Nutrition*, 44, pp. 260-265.

16. Tsagarakis, N.J., Drygiannakis, I., Batistakis, A.G., Kolios, G. and Kouroumalis, E.A., 2010, "A Concentration-Dependent Effect of Ursodeoxycholate on Apoptosis and Caspases Activities of HepG2 Hepatocellular Carcinoma Cells," *European Journal of Pharmacology*, 640 (1-3), pp. 1-7.

17. Yin, Y., Chen, W., Tang, C., Ding, H., Jang, J., Weng, M., Cai, Y. and Zou, G., 2011, "NF-κB, JNK and p53 Pathways are Involved in Tubeimoside-1-Induced Apoptosis in HepG2 Cells with Oxidative Stress and G2/M Cell Cycle Arrest," *Food and Chemical Toxicology*, 49 (12), pp. 3046-3054.

18. Zelig, U., Kapelushnik, J., Moreh, R., Mordechai, S. and Nathan, I., 2009, "Diagnosis of Cell Death by Means of Infrared Spectroscopy," *Biophysical journal*, 97 (7), pp. 2107-2114.

19. Machana, S., Weerapreeyakul, N., Barusrux, S., Thumanu, K. and Tanthanuch, W., 2012, "FTIR Microspectroscopy Discriminates Anticancer Action on Human Leukemic Cells by Extracts of *Pinus kesiya; Cratoxylum formosum* ssp. *pruniflorum* and melphalan," *Talanta*, 93, pp. 371-382.

20. Gasparri, F. and Muzio, M., 2003, "Monitoring of Apoptosis of HL60 Cells by Fourier-Transform Infrared Spectroscopy," *Biochemical Journal*, 369 (2), pp. 239-248.

21. Pamok, S., Vinitketkumnuen, S.S.U. and Saenphet, K., 2012, "Antiproliferative Effect of *Moringa oleifera* Lam. and *Pseuderanthemum palatiferum* (Nees) Radlk Extracts on the Colon Cancer Cells," *Journal of Medicinal Plants Research*, 6 (1), pp. 139-145.

22. Majno, G. and Joris, I., 1995, "Apoptosis, Oncosis, and Necrosis. An Overview of Cell Death," *The American journal of pathology*, 146 (1), pp. 3-15.

23. MacFarlane, M. and Williams, A.C., 2004. "Apoptosis and Disease: a Life or Death Decision: Conference and Workshop on Apoptosis and Disease," *EMBO Reports*, 5 (7), pp. 674-678.

24. Kongprasom, U., Sukketsiri, W., Chonpathompikunlert, P., Sroyraya, M., Sretrirutchai, S. and Tanasawet, S., 2019, "*Pseuderanthemum palatiferum* (Nees) Radlk Extract Induces Apoptosis via Reactive Oxygen Species-mediated Mitochondria-dependent Pathway in A549 Human Lung Cancer Cells," *Tropical Journal of Pharmaceutical Research*, 18 (2), pp. 287-294.

25. Plaimee, P., Weerapreeyakul, N., Thumanu, K., Tanthanuch, W. and Barusrux, S., 2014, "Melatonin Induces Apoptosis through Biomolecular Changes, in SK-LU-1 Human Lung Adenocarcinoma Cells," *Cell Proliferation*, 47 (6), pp. 564-577.

26. Lamberti, A., Sanges, C. and Arcari, P., 2010, "FT-IR Spectromicroscopy of Mammalian Cell Cultures During Necrosis and Apoptosis Induced by Drugs," *Journal of Spectroscopy*, 24 (5), pp. 535-546.

27. Liu, K.Z. and Mantsch, H., 2001, "Apoptosis-induced Structural Changes in Leukemia Cells Identified by IR Spectroscopy," *Journal of Molecular Structure*, 565, pp. 299-304.

28. Dewson, G. and Kluck, R.M., 2009, "Mechanisms by Which Bak and Bax Permeabilise Mitochondria During Apoptosis," *Journal of Cell Science*, 122 (16), pp. 2801-2808.

29. Mohlenhoff, B., Romeo, M., Diem, M. and

Wood, B.R., 2005, "Mie-type Scattering and Non-Beer-Lambert Absorption Behavior of Human Cells in Infrared Microspectroscopy," *Biophysical Journal*, 88 (5), pp. 3635-3640.

30. Verrier, S., Notingher, I., Polak, J. and Hench, L., 2004, "In Situ Monitoring of Cell Death Using Raman Microspectroscopy," *Biopolymers: Original Research on Biomolecules*, 74 (1-2), pp. 157-162.

31. Pocasap, P., Weerapreeyakul, N. and Thumanu, K., 2019, "Alyssin and Iberin in Cruciferous Vegetables Exert Anticancer Activity in HepG2 by Increasing Intracellular Reactive Oxygen Species and Tubulin Depolymerization," *Biomolecules and Therapeutics*, 27 (6), pp. 540-552.

32. Marcelli, A. and Cinque, G., 2019, "Synchrotron Radiation InfraRed microspectroscopy and Imaging in the Characterization of Archaeological Materials and Cultural Heritage Artefacts," *The Contribution of Mineralogy to Cultural Heritage*, 20, pp. 411-444.